The activity and dynamical evolution of quasi-hilda asteroid (457175) 2008 GO98☆

E. García-Migani [*], R. Gil-Hutton

Grupo de Ciencias Planetarias, Departamento de Geofísica y Astronomía, Facultad de Ciencias Exactas, Físicas y Naturales, Universidad Nacional de San Juan - CONICET, Av. José I. de la Roza 590 (O), J5402DCS Rivadavia, San Juan, Argentina

ARTICLE INFO

ABSTRACT

The quasi-Hilda asteroid (457175) 2008 GO98 was found in a previous study as a good candidate to show cometary activity since it seems to come from the Centaurs region. The object was observed in the post-perihelion arc of its orbit during several runs between September 2016 and June 2017 with the $2.15\,m$ telescope at Complejo Astronómico El Leoncito (CASLEO) in San Juan, Argentina. The images obtained were analyzed and the object was observed active with a small coma that grew in size and brightness as the object moved away from the perihelion of the orbit, while in June 2017 it also showed a small tail. In order to get an estimation of the diameter of the nucleus the coma contribution has been calculated and subtracted to find values of $15.5 \pm 4.0\,km$ and $20.1 \pm 5.4\,km$ for albedos of $p_R = 0.13$ and $p_R = 0.069$, respectively. To understand the recent dynamical evolution of (457175) 2008 GO98, the orbit of the object and those of 100 clones were numerically integrated backward and forward in time for 30000 yr. The dynamical evolution confirms that this object is a recent incomer from the outer region of the solar system but it will return to this region in a short period of time indicating that its present dynamical state is rather transient.

1. Introduction

Jupiter-family comets (JFCs) are objects that reach the inner solar system after a dynamical evolution that took them from the transneptunian region, pass through the external planets zone where they behaved as Centaurs, and finish their journey as objects characterized by orbits inside Jupiter's showing activity when they approach the perihelion of their orbits. In their final state as JFCs these objects have unstable orbits that are strongly affected by the gravitational perturbation of Jupiter (Fernandez, 1980; Duncan et al., 1995; Levison and Duncan, 1997).

Several JFCs arrived the inner region of the solar system to stay in an unstable 3 : 2 mean motion resonance with Jupiter. The comets were called *quasi-Hilda comets* (QHCs) by Kresak (1979) and currently there are several objects in this region which also have undergone a temporary satellite capture by Jupiter during their passage from outside to inside the orbit of this planet (i.e., Ohtsuka et al., 2008). This resonance is also populated by a group of asteroids in stable orbits called the Hilda group (Schubart, 1968, 1982; 1991; Nesvorný and Ferraz-Mello, 1997;

Ferraz-Mello et al., 1998) with semimajor axes in the range $3.7 \leq a \leq 4.2\,au$, eccentricities $e \leq 0.3$, inclinations $i \leq 20^o$, and a critical argument for the resonance librating around 0° (Zellner et al., 1985).

Unfortunately, the quasi-Hilda region is also visited by Hilda objects escaping from the stable region of the mean motion resonance making difficult to differentiate between these objects and QHCs without a study of their orbital evolution. Toth (2006) gave an update of the QHCs in this region, found new members, and identified 23 objects that could be dormant or extinct comet nuclei, while Gil-Hutton and García-Migani (2016) searched for new QHCs candidates that have recently arrived at this zone from the Centaur region and found 11 objects that show a dynamical behavior that is expected for comets injected in the quasi-Hilda region from outside the orbit of Jupiter. A possible method to confirm their cometary nature is to search for signals of activity of some kind that indicate mass loss triggered by sublimation of volatile material.

Then, we started an observational campaign from Complejo Astronómico El Leoncito (CASLEO), Argentina, to search for activity on the QHCs candidates listed by Gil-Hutton and García-Migani (2016). Recently, one of these quasi-hilda objects, (457175) 2008 GO98, was

reported as active on July 2017 by (Leonard et al., 2017) with a coma of $7 - 8 \, arcsec$ in diameter and a tail, so it is an excellent candidate to study its activity and dynamical evolution.

In this paper we present results for this object indicating that it was active since few months before the Leonard et al. detection and we also make an analysis of its dynamical evolution. The data acquisition, the reduction process and the observational results are explained in Sections 2 and 3. In Section 4 we analyze the dynamical evolution of (457175) 2008 GO98, and the summary and conclusions are given in Section 5.

2. Observations

The quasi-hilda object (457175) 2008 GO98 was discovered by the Spacewatch Team at Kitt Peak on April 8, 2008. It has a period of $7.89 \, yr$ and a Tisserand parameter with Jupiter of $T_J = 2.927$. Its orbital parameters were taken from the JPL Horizon Database[1] and are listed in Table 1. The last perihelion passage of this object was August 21, 2016.

The object was observed in several runs between September 5, 2016 and June 25, 2017, with the $2.15 \, m$ telescope at Complejo Astronómico El Leoncito (CASLEO) in San Juan, Argentina. For all the observations a focal reducer was used obtaining a plate scale of $33.9 \, arcsec \, mm^{-1}$ and a circular useful field of $9 \, arcmin$. The detector is a thinned back-illuminated, coated CCD with 2048×2048 square pixels with size of $13.5 \, \mu m$ and installed on a dewar cooled with liquid nitrogen, resulting in a negligible dark current ($< 1 \, e^-/h/pixel$). The CCD was configured with a 2×2 on-chip binning resulting in a scale of $0.9 \, arcsec/pixel$. Although, in this way we lose resolution to resolve a potential coma of the object, we gain signal-to-noise which is observationally advantageous since it is a faint object for our telescope. Finally, a broadband R filter of the Johnson-Cousins system was also used in order to try to detect a dust coma and/or tail.

All the images were corrected by bias and flat-fielding in the standard way using tasks and scripts available in *IRAF*. Each night, 10 zero-exposure frames and 10 twilight flat-fields were taken and averaged to obtain final images with enough good signal-to-noise ratio. The flat-fields exposure times were long enough to avoid any shutter effect. In order to obtain the best possible quality in the images of the object we avoid the use of removal algorithms to correct for cosmic rays, and preferred to reject any image with cosmic rays near the target. The observation conditions were good, except the first part of the night of the second run (March 29, 2017) which was affected by some cirrus. The images acquired in those conditions were discarded and only six individual images with enough good quality were used from that night.

A summary of the observational circumstances for all the nights are shown in Table 2, where the heliocentric distance (r), the geocentric distance (Δ), the phase angle (α), the true anomaly (f) and the number of individual images taken in each night are listed. In Fig. 1 the orbit of (457175) 2008 GO98 and Jupiter are shown, where the perihelia are marked with crosses and the positions of the object when it was observed are indicated by squares.

To avoid elongated images the exposure time of the individual images

Table 1
Orbital parameters of (457175) 2008 GO98 for the Epoch Dec 04, 2015 TDB.

Element	Value	Uncertainty (1σ)
Semimajor axis (au)	3.9646070	3.6988×10^{-7}
Eccentricity	0.2809973	3.9189×10^{-7}
Inclination (deg)	15.56866	2.9514×10^{-5}
Ascending node (deg)	192.60859	4.6882×10^{-5}
Argument of pericenter (deg)	53.28665	1.2159×10^{-4}
Mean anomaly (deg)	327.17517	8.5168×10^{-5}

Table 2
Observing circumstances for (457175) 2008 GO98.

Date	r^a	Δ^b	α^c	f^d	n^e
0 UT	au	au	deg	deg	
2016-Sep-05	2.851	3.111	18.8	3.2	$16 \times 60s$
2016-Sep-06	2.851	3.122	18.7	3.4	$30 \times 60s$
2017-Mar-29	3.072	3.475	16.1	47.9	$6 \times 70s$
2017-Mar-30	3.074	3.465	16.2	48.1	$20 \times 75s$
2017-Jun-24	3.254	2.572	15.0	64.3	$10 \times 360s$
2017-Jun-25	3.257	2.563	14.8	64.5	$10 \times 360s$

[a] Heliocentric distance; [b] geocentric distance; [c] phase angle; [d] true anomaly; [e] number of individual images and their exposure times.
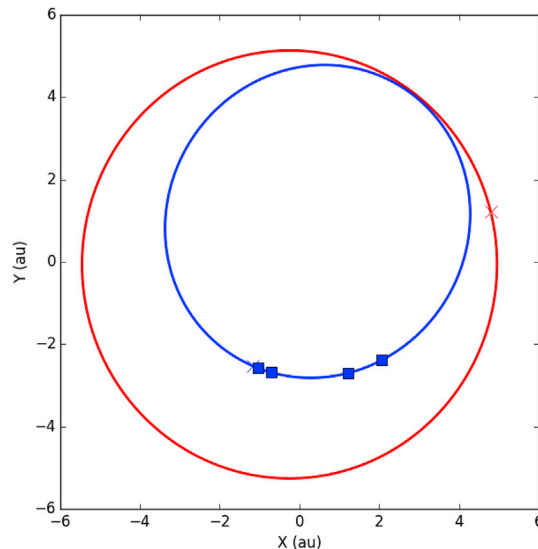

Fig. 1. Orbit of (457175) 2008 GO98 in blue with the positions of our observations in 2016 and 2017 marked with blue squares. **The orbit of Jupiter is plotted in red. Both Jupiter and 2008 GO98 perihelion are indicated with crosses.** (For interpretation of the references to color in this figure legend, the reader is referred to the Web version of this article.)

was limited by the angular velocity of the object and the requirement that it does not move more than half a pixel during the exposure. Then, to obtain better signal-to-noise ratio we co-add the individual images centering them in the photocenter of the object using the task *imcntr* of the *IRAF* package.

The first two nights we had some problems with the Moon due to its proximity with the object, which produced some troublesome artifacts like bright patterns and a step background gradient in the CCD. The first night the Moon was 20% illuminated and at an angular distance from the object of 16°, while the second night the Moon was illuminated 26% and at an angular distance of 7.3^o. To deal with this undesirable effects we had to resort to some processing techniques to fit the illumination gradient and to substract it from the images. The other nights it was not necessary to apply any correction.

3. Results

3.1. Looking for activity

The observations of (457175) 2008 GO98 taken in September 2016 at first glance did not show signals of cometary activity, but it is possible that a compact unresolved coma could dominate the total brightness of a faint active object masking its cometary activity (Jewitt, 1991). Bearing this in mind and in order to detect any signs of activity, we decided to compare the brightness profile of the object with stellar profiles in the

same field since the point spread function (PSF) of an extended object, like an active comet, has a broader profile than that of a stellar object. This technique is widely used to detect signs of mass loss in objects of the solar system, while Luu (1992) applied this technique to detect cometary activity in near-Earth asteroids, and Licandro et al. (2000); Mazzotta Epifani et al. (2008); Fitzsimmons et al. (2005) do the same for Jupiter-family comets. There are also several examples of the application of this method to detect activity in Centaurs and transneptunian objects (Perna et al., 2013; Mazzotta Epifani et al., 2014; 2017).

The profile for 2008 GO98 was obtained fitting a gaussian to the values of each pixel in two orthogonal directions and normalizing the flux to a value of 1 at the photocenter taking as reference the background level. The same was done for several stars near the object which were combined to obtain the comparison stellar profile. In both cases we used Python functions to make the fits.

Figs. 2 and 3 show the images of 2008 GO98 obtained in September 5 and 6, 2016, respectively, and also the comparison between the profiles of the object and the stellar PSF. In both nights the profiles of 2008 GO98 are broader than the stellar PSF indicating the possibility that it could be active with a small coma. On those dates the object was very near the perihelion (the true anomaly was $\sim 3^o$) and it was in the post-perihelion arc of its orbit.

Fig. 4 shows the image and profiles for March 28, 2017. On this night the number of useful images was limited because the object passed very near of two background stars. Again, the image of 2008 GO98 is at left and the profiles at right. It could be observed that the object's profile is broader than the stellar PSF, and even broader than the object profile in the previous observations. In fact the profile shows a significant asymmetry. Looking carefully the image of the object it is possible to detect a subtle elongated coma in the anti-solar direction which produces the asymmetry in the observed profile. The same thing happens with the observations taken in March 29, 2017. Because the images taken in March 28, 2017 allow to identify that the object is active without any doubt, for the remaining observations it was decided to replace the comparison of profiles with a contour plot of the object in order to confirm the presence of a coma. The contour plot shown in Fig. 5 indicates that there is an asymmetric structure in the image with an elongation towards the anti-solar direction.

The results of the last observing run (June 24 and 25, 2017) are shown in Figs. 6 and 7. Surprisingly, 10 months after its perihelion passage and with a true anomaly larger than 60°, the object showed its cometary nature in a clear and unequivocal way, presenting also a small tail in Fig. 7. This observed activity several months after its perihelion passage could be related with a thermal inertia effect observed in comets that produce the maximum of activity some time after the perihelion passage (Kelley et al., 2013; Schleicher et al., 1998; Knight and Schleicher, 2013).

3.2. Nucleus

In order to get an estimation of the size of the nucleus of 2008 GO98, we use the images taken in September 05, 2016 because they show a less developed coma. Assuming a standard steady-state coma, it is possible to infer the integrated coma magnitude and its contribution to the total brightness, which allows us to derive the contribution of the nucleus and its radius. This method, was developed by Jewitt and Danielson (1984) to constrain the brightness of the coma of comet Halley at large heliocentric distances and it was used by Mazzotta Epifani et al. (2007) to characterize Jupiter family comets with low activity.

The coma magnitude m_{coma} within a circle of projected radius ρ in arc-seconds could be expressed as:

$$m_{coma} = \Sigma_R(\rho) - 2.5 log\left(2\pi\rho^2\right), \tag{1}$$

where $\Sigma_R(\rho)$ is the surface brightness at a projected distance ρ in magnitudes per square arc-second. Then, once m_{coma} was estimated we can calculate which proportion of the total brightness comes from the coma by:

$$\frac{F_{coma}}{F} = 10^{-0.4(m_{coma}-m)}, \tag{2}$$

where F_{coma}, F, m_{coma} and m are the flux of the coma, the total flux, the coma magnitude and the total magnitude of the object, respectively.

The value of ρ was chosen in order to include at least the 90% of the photometric light of the object, which was determined using the *psfmeasure* task of IRAF. Then from Eqs. (1) and (2) we get $\frac{F_{coma}}{F} = 0.67$, which indicates that the coma contamination is considerable. Once we got this estimation, the standard magnitude of the nucleus, $m_{nucleus}$, is:

$$m_{nucleus} = m - 2.5 \log\left(1 - \frac{F_{coma}}{F}\right). \tag{3}$$

In the case of 2008 GO98 we found an estimation for the total standard magnitude $m = 16.7 \pm 0.1$ and then we get $m_{nucleus} = 17.9$, this value give us an absolute magnitude $H = 13.15$ which is in good agreement with the value in the JPL Horizon Database($H = 13.3$). This value for the magnitude of the nucleus could be used to derive its size using the standard technique introduced by Russell (1916) and reformulated for a spherical object by Jewitt (1991). The relation between the magnitude of a spherical object and its radius is:

$$p_R\Phi(\alpha)a^2 = 2.238 \times 10^{22}r^2\Delta^2 10^{0.4(m_\odot - m_{nucleus})}, \tag{4}$$

where p_R is the geometric albedo, $\Phi(\alpha)$ the phase function ($\Phi(\alpha) = 10^{-0.4(\alpha\beta)}$, α is the phase angle and β the phase coefficient), a is the radius of the object in meters, r and Δ are the heliocentric and geocentric distances in astronomical units, and $m_\odot = -27.1$ and $m_{nucleus}$ are the magnitudes of the Sun and the object in the R-filter, respectively.
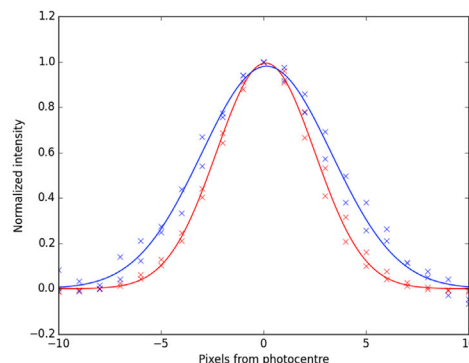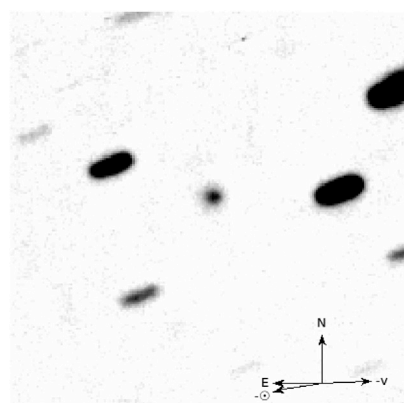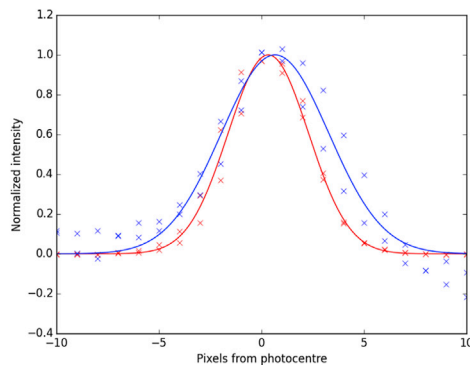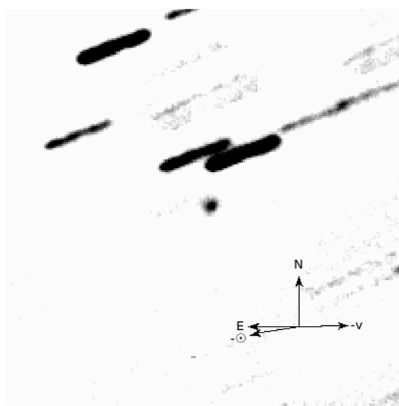

Fig. 2. *(Left)* Result of co-adding 16 images with an individual exposure time of 30 s taken in September 05, 2016. The object in the center of the image is (457175) 2008 GO98. North is up and East left, the arrow with the $-\odot$ symbol indicates the antisolar direction, and that with $-v$ the direction opposite to the object's heliocentric velocity vector. The image is 180 arcsec per side. *(Right)* The profiles of 2008 GO98 (blue) and the stellar PSF for comparison (red). (For interpretation of the references to color in this figure legend, the reader is referred to the Web version of this article.)
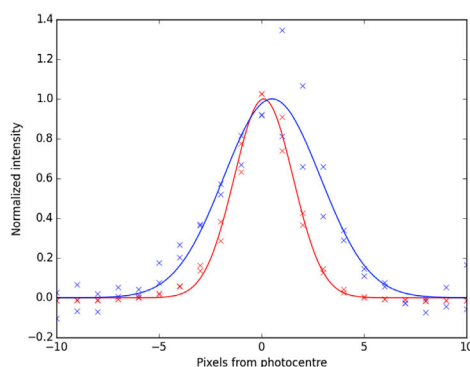
Fig. 3. *(Left)* Result of co-adding 6 images with an individual exposure time of 70 s taken in September 06, 2016. The object in the center of the image is (457175) 2008 GO98. North is up and East left, the arrow with the $-\odot$ symbol indicates the antisolar direction, and that with $-v$ the direction opposite to the object's heliocentric velocity vector. The image is 180 arcsec per side. *(Right)* The profile of 2008 GO98 (blue) and the stellar PSF for comparison (red). (For interpretation of the references to color in this figure legend, the reader is referred to the Web version of this article.)
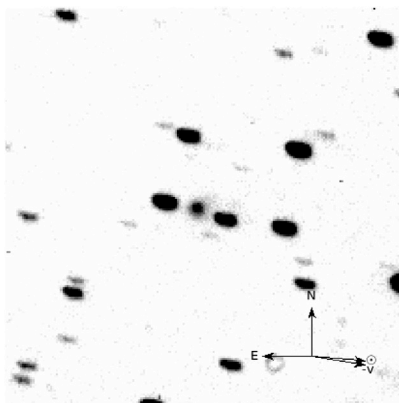

Fig. 4. *(Left)* Result of co-adding 6 images with an individual exposure time of 70 s taken in March 29, 2017. The object in the center of the image is (457175) 2008 GO98. North is up and East left, the arrow with the $-\odot$ symbol indicates the antisolar direction, and that with $-v$ the direction opposite to the object's heliocentric velocity vector. The image is 180 arcsec per side. *(Right)* The profile of 2008 GO98 (blue) and the stellar PSF for comparison (red). (For interpretation of the references to color in this figure legend, the reader is referred to the Web version of this article.)
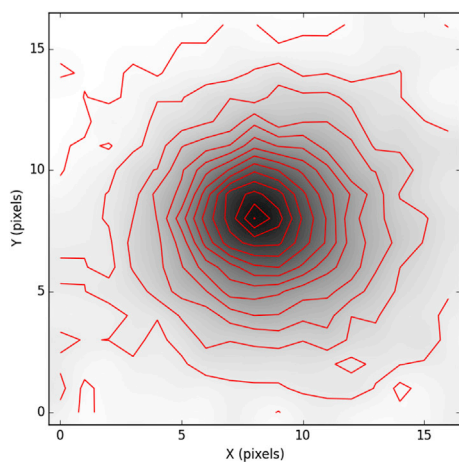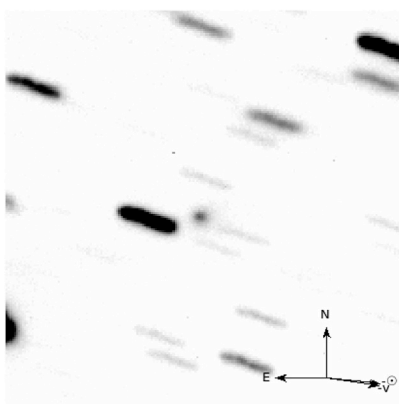

Fig. 5. *(Left)* Result of co-adding 20 images with an individual exposure time of 75 s taken in March 30, 2017. The object in the center of the image is (457175) 2008 GO98. North is up and East left, the arrow with the $-\odot$ symbol indicates the antisolar direction, and that with $-v$ the direction opposite to the object's heliocentric velocity vector. The image is 180 arcsec per side. *(Right)* The profile of 2008 GO98 (blue) and the stellar PSF for comparison (red). (For interpretation of the references to color in this figure legend, the reader is referred to the Web version of this article.)

The diameter of the object could be found using Eq. (4) but we need to make assumptions about the values of the phase coefficient (β) and the albedo (p_R). While the present orbital elements of 2008 GO98 indicate that it belongs to the JFCs population, it would seem that it recently arrived to the quasi-hilda region from the Centaur zone (Gil-Hutton and García-Migani, 2016). Then, the best guess for β and p_R in this case is a mean value between those corresponding to these populations. While the values of β estimated for periodic comets fall generally in the interval $0.04 \geq \beta \geq 0.03\ mag\ deg^{-1}$ Jewitt and Danielson (1984); Lamy et al. (2004), for some objects in the Centaur population the estimated values are slightly higher: Jewitt (2009) used $\beta = 0.10\ mag\ deg^{-1}$ for his study

of active centaurs while Peixinho et al. (2004) proposed $\beta = 0.11\ mag\ deg^{-1}$. In the case of the albedo the value usually assumed for JFCs is $p_R = 0.04$, while for the Centaur population the albedo is in the range of $0.025 \leq p_R \leq 0.260$ with a mean value of $p_R \sim 0.069 \pm 0.039$ (Duffard et al., 2014).

Then, following the same procedure used by Mazzotta Epifani et al. (2017) in Fig. 8 the two curves show the radius in function of the albedo for $\beta = 0.035\ mag\ deg^{-1}$ and $0.110\ mag\ deg^{-1}$, and the vertical lines indicate the mean albedos assumed for JFCs, Centaurs, and $p_R = 0.13$ which is the albedo of two active Centaurs (Chiron and 29P/Schwassmann-Wachmann 1 Cruikshank and Brown, 1983; Bus et al., 1989).
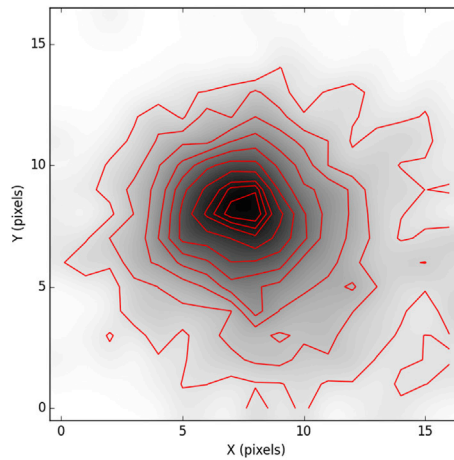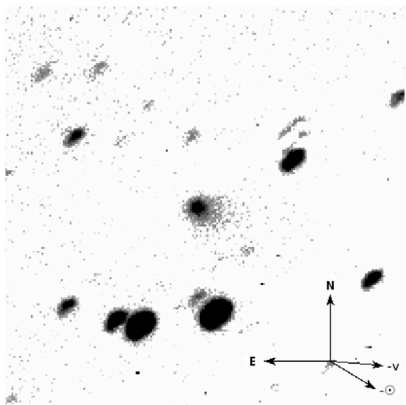
Fig. 6. *(Left)* Result of co-adding 10 images with an individual exposure time of 360 s taken in June 24, 2017. The object in the center of the image is (457175) 2008 GO98. North is up and East left, the arrow with the $-\odot$ symbol indicates the antisolar direction, and that with $-v$ the direction opposite to the object's heliocentric velocity vector. The image is 180 arcsec per side. *(Right)* The profile of 2008 GO98 (blue) and the stellar PSF for comparison (red). (For interpretation of the references to color in this figure legend, the reader is referred to the Web version of this article.)
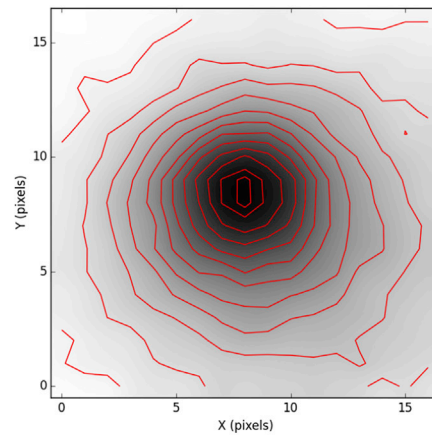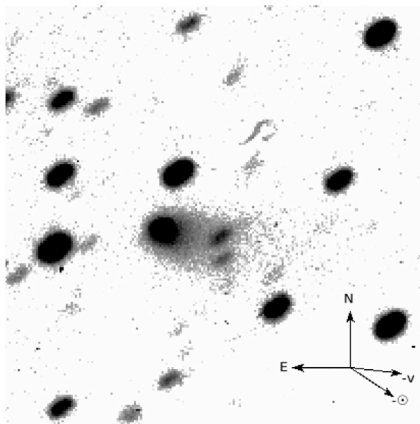

Fig. 7. *(Left)* Result of co-adding 10 images with an individual exposure time of 360 s taken in June 25, 2017. The object in the center of the image is (457175) 2008 GO98. North is up and East left, the arrow with the $-\odot$ symbol indicates the antisolar direction, and that with $-v$ the direction opposite to the object's heliocentric velocity vector. The image is 180 arcsec per side. *(Right)* The profile of 2008 GO98 (blue) and the stellar PSF for comparison (red). (For interpretation of the references to color in this figure legend, the reader is referred to the Web version of this article.)

Taking mean values, the estimated diameter of 2008 GO98 is $15.5 \pm 4.0\ km$ or $20.1 \pm 5.4\ km$ for $p_R = 0.13$ and $p_R = 0.069$, respectively.

4. Dynamical evolution

To investigate the recent dynamical evolution of 2008 GO98, we numerically integrate its orbit backwards and forwards in time for 30000 yr (See Table 1 for the elements of the initial orbit), and we also integrated 100 clones with uniform distributed orbital elements centered on its current orbit with a dispersion of 10^{-3} of each element. For this purpose, we used a Bulirsch-Stoer integrator with a step size of 1 day, adopted accuracy of 10^{-12}, and all the planets from Mercury to Neptune included.

The evolution of the semimajor axis, and the perihelion and aphelion distances of 2008 GO98 are shown in Fig. 9. The simulation results show that the orbit of 2008 GO98 was strongly perturbed by Jupiter: the object behaves as Centaur until the year ≈ -1840 when it crosses Jupiter's orbit to enter the inner solar system and becomes a quasi-hilda object in the year ≈ 2000. Later, in the year ≈ 5788 2008 GO98 crosses again Jupiter's orbit to return to the Centaur zone when the semimajor axis and aphelion of its orbit jump to larger values. Then, this object behaves as quasi-hilda during a very short period of $\approx 7000\ yr$.

Analyzing the behavior of the clones during the integration allow us to confirm that 2008 GO98 is in an orbit which is dynamically unstable on very short time-scales. The spread of the main orbital parameters of
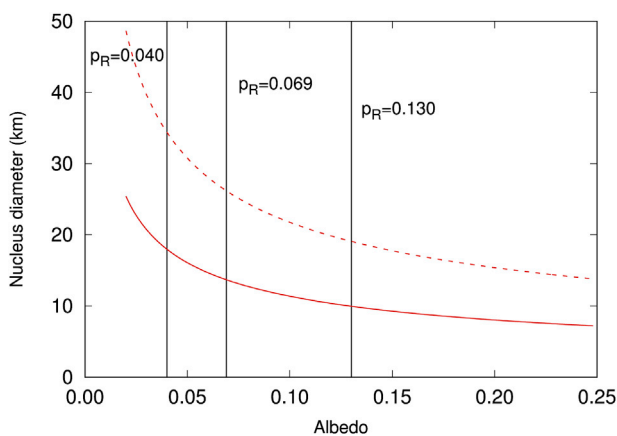

Fig. 8. Diameter of the nucleus of 2008 GO98 in function of the albedo. The red curve corresponds to values obtained with a phase coefficient of $\beta = 0.11\ mag\ deg^{-1}$, while the red dashed one is for $\beta = 0.035\ mag\ deg^{-1}$. The vertical lines indicate albedos of 0.04, 0.069, and 0.13. (For interpretation of the references to color in this figure legend, the reader is referred to the Web version of this article.)
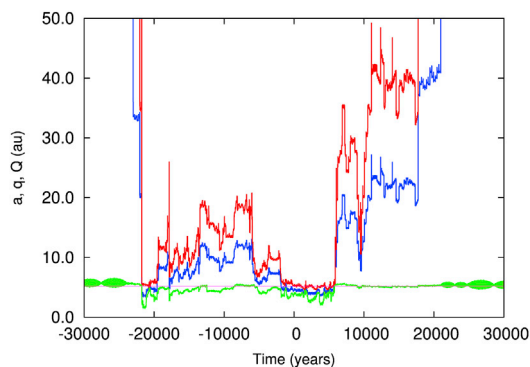
Fig. 9. Dynamical evolution of the semimajor axis (blue), perihelion (green), and aphelion (red) distances for (457175) 2008 GO98 during the numerical integration. Jupiter's semimajor axis is also shown in pink. (For interpretation of the references to color in this figure legend, the reader is referred to the Web version of this article.)

the cloud of clones expands by a factor of 2 in less than 10 *yr* into the past and $\approx 20\,yr$ into the future, indicating that the orbit has a strongly chaotic nature.

The evolution of the mean semimajor axis, perihelion distance, eccentricity and inclination of the clones are shown in Fig. 10. The frequent encounters of the clones with Jupiter lead to a divergence of their orbits allowing only a statistical analysis of their evolution. These results indicate that 2008 GO98 has a high probability of being a centaur that was occasionally disturbed by Jupiter to temporarily become a quasi-hilda during a very short time in which it was detected as an active object. This chaotic behavior is rather common among the centaur population since these objects have frequent encounters with Jupiter and Saturn.

We also obtain the time-averaged distribution of the clones as a function of the aphelion (Q) and perihelion (q) distances for the backward and forward integrations (Fig. 11). We can see in this figure the clear influence of Jupiter on the evolution of the orbit indicated by horizontal strips of high probability at $q =\sim 5.2\,au$ in both cases, and also a less important influence of Saturn in the forward integration indicated
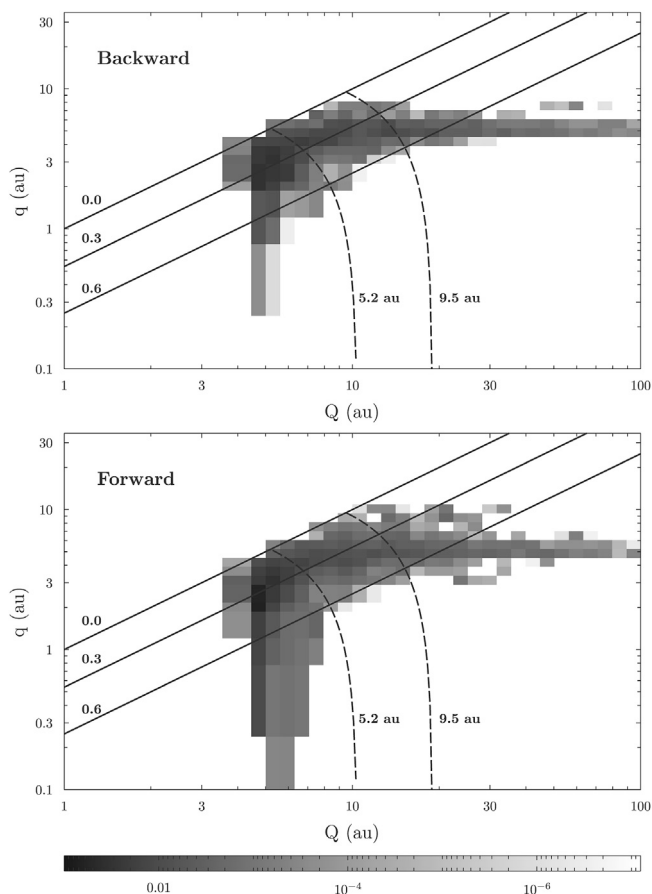

Fig. 11. Probability distribution per square au in (Q, q) space for the clones of 2008 GO98 in the backward and forward integrations. Continuous black lines indicate eccentricities of 0.0, 0.3, and 0.6, and dashed lines indicate semimajor axes of 5.2 and 9.5 au, **Jupiter and Saturn locations**.
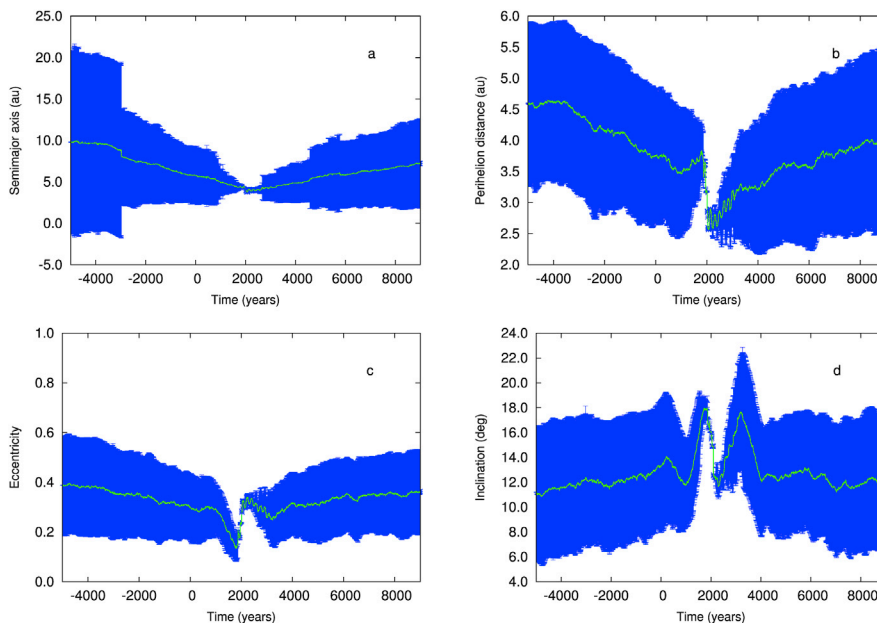

Fig. 10. Orbital evolution of the 100 clones of (457175) 2008 GO98 for the semimajor axis (a), perihelion distance (b), eccentricity (c), and inclination (d). The mean value is indicated in green while one standard deviation for each point is indicated in blue. (For interpretation of the references to color in this figure legend, the reader is referred to the Web version of this article.)

as a high probability region at $q =\sim 9.5 \, au$.

5. Conclusions

In Gil-Hutton and García-Migani (2016) we found 11 objects whose dynamical evolution show that they could have recently come from the outer solar system and several of them have a good chance of being active. One of them, the quasi-hilda object (457175) 2008 GO98, passed the perihelion of its orbit on August 21, 2016, offering a good opportunity to search for activity. The object was observed in several runs between September 5, 2016 and June 25, 2017, with the 2.15 m telescope at Complejo Astronómico El Leoncito (CASLEO) in San Juan, Argentina.

The observations made in September 2016 at a first glance did not show evidence of activity but a comparison of the photometric profile with a stellar PSF show a clear widening, evidencing the presence of a coma. The object becomes more active in the following observing runs and in June 2017 it was visible in the images a small tail. Surprisingly, the object increases its activity for increasing true anomaly in spite that the heliocentric distance was greater in June 2017 than in September 2016 when it was near its perihelion.

In order to get an estimation of the nucleus size we use the images taken in the first run when the coma contamination was apparently smaller. The value obtained for the nucleus diameter was $15.5 \pm 4.0 \, km$ for $p_R = 0.13$ and $20.1 \pm 5.4 \, km$ for $p_R = 0.069$. These values are higher than one would expect for a typical JFC but it is in agreement with the size obtained by Mazzotta Epifani et al. (2017) for the active Centaur C/2011 P2 (PANSTARRS). On the other hand it is also possible that the coma contamination is being underestimated by the method used and hence the nucleus brightness was overestimated. Therefore these values must be considered only as a first-order estimation for the nucleus size.

The dynamical evolution of 2008 GO98 shows that its present orbit is transient and the object will return to the Centaur region after a short period inside the orbit of Jupiter. Since this object was observed active its surface suffered a thermal process that triggered the activity and broke the irradiation crust, producing a resurfacing process and a likely change of the surface color. Since 2008 GO98 will return to the Centaur region after this processing of its surface, it could be an example of the dynamical process proposed by Melita and Licandro (2012) to help to explain the color bimodality of the Centaur population. These authors found that the objects that are less red do not penetrate too much into the inner solar system and viceversa, indicating that the dynamics could be one of the factors that determine the surface color in addition to other factors like their size, collisional processes, intrinsic composition, etc.

In the case of 2008 GO98, when this object return to the Centaur region it will be a new member of the less red group confirming the proposal of Melita and Licandro (2012).

Acknowledgements

References

Bus, S.J., Bowell, E., Harris, A.W., Hewitt, A.V., 1989. 2060 Chiron - CCD and electronographic photometry. Icarus 77, 223–238.

Cruikshank, D.P., Brown, R.H., 1983. The nucleus of comet P/Schwassmann-Wachmann 1. Icarus 56, 377–380.

Duffard, R., Pinilla-Alonso, N., Santos-Sanz, P., Vilenius, E., Ortiz, J.L., Mueller, T., Fornasier, S., Lellouch, E., Mommert, M., Pal, A., Kiss, C., Mueller, M., Stansberry, J.,

Delsanti, A., Peixinho, N., Trilling, D., 2014. "TNOs are Cool": a survey of the trans-Neptunian region. XI. A Herschel-PACS view of 16 Centaurs. A&A 564, A92.

Duncan, M.J., Levison, H.F., Budd, S.M., 1995. The dynamical structure of the kuiper belt. AJ 110, 3073.

Fernandez, J.A., 1980. On the existence of a comet belt beyond Neptune. MNRAS 192, 481–491.

Ferraz-Mello, S., Nesvorny, D., Michtchenko, T.A., 1998. Chaos, diffusion, escape and permanence of resonant asteroids in gaps and groups. In: Lazzaro, D., Vieira Martins, R., Ferraz-Mello, S., Fernandez, J. (Eds.), Solar System Formation and Evolution, vol. 149, p. 65 of Astronomical Society of the Pacific Conference Series.

Fitzsimmons, A., Lowry, S.C., Snodgrass, C., 2005. Comet observations [F65 haleakala-faulkes telescope north]. Minor Planet Circulars 53903.

Gil-Hutton, R., García-Migani, E., 2016. Comet candidates among quasi-Hilda objects. A&A 590, A111.

Jewitt, D., 1991. Cometary photometry. In: Newburn Jr., R.L., Neugebauer, M., Rahe, J. (Eds.), IAU Colloq. 116: Comets in the Post-Halley Era, vol. 167. Astrophysics and Space Science Library, pp. 19–65.

Jewitt, D., 2009. The active centaurs. AJ 137, 4296–4312.

Jewitt, D., Danielson, G.E., 1984. Charge-coupled device photometry of Comet P/Halley. Icarus 60, 435–444.

Kelley, M.S., Fernández, Y.R., Licandro, J., Lisse, C.M., Reach, W.T., A'Hearn, M.F., Bauer, J., Campins, H., Fitzsimmons, A., Groussin, O., Lamy, P.L., Lowry, S.C., Meech, K.J., Pittichová, J., Snodgrass, C., Toth, I., Weaver, H.A., 2013. The persistent activity of Jupiter-family comets at 3-7 AU. Icarus 225, 475–494.

Knight, M.M., Schleicher, D.G., 2013. The highly unusual outgassing of Comet 103P/Hartley 2 from narrowband photometry and imaging of the coma. Icarus 222, 691–706.

Kresak, L., 1979. In: Gehrels, T. (Ed.), Asteroids. University of Arizona Press, Tucson, pp. 289–309.

Lamy, P.L., Toth, I., Fernandez, Y.R., Weaver, H.A., 2004. In: Festou, M.C., Keller, H.U., Weaver, H.A. (Eds.), Comets II. University of Arizona Press, pp. 223–264.

Leonard, G.J., Christensen, E.J., Fuls, D.C., Gibbs, A.R., Grauer, A.D., Johnson, J.A., Kowalski, R.A., Larson, S.M., Matheny, R.G., Seaman, R.L., Shelly, F.C., Williams, G.V., 2017. Cometary Activity in (457175) 2008 GO98. Minor Planet Electronic Circulars 2017.

Levison, H.F., Duncan, M.J., 1997. From the kuiper belt to Jupiter-family comets: the spatial distribution of ecliptic comets. Icarus 127, 13–32.

Licandro, J., Tancredi, G., Lindgren, M., Rickman, H., Hutton, R.G., 2000. CCD photometry of cometary nuclei, I: observations from 1990-1995. Icarus 147, 161–179.

Luu, J.X., 1992. High resolution surface brightness profiles of near-earth asteroids. Icarus 97, 276–287.

Mazzotta Epifani, E., Palumbo, P., Capria, M.T., Cremonese, G., Fulle, M., Colangeli, L., 2007. The distant activity of short-period comets - I. MNRAS 381, 713–722.

Mazzotta Epifani, E., Palumbo, P., Capria, M.T., Cremonese, G., Fulle, M., Colangeli, L., 2008. The distant activity of short period comets - II. MNRAS 390, 265–280.

Mazzotta Epifani, E., Perna, D., Dotto, E., Palumbo, P., Dall'Ora, M., Micheli, M., Ieva, S., Perozzi, E., 2017. Nucleus of the active centaur C/2011 P2 (PANSTARRS). A&A 597, A59.

Mazzotta Epifani, E., Perna, D., Licandro, J., Dall'Ora, M., Palumbo, P., Dotto, E., Barucci, M.A., Brucato, J.R., Della Corte, V., Tozzi, G.P., 2014. Blending the distinctions among groups of minor bodies: a portrait of the Centaur-comet "transition" object P/2010 C1 (Scotti). A&A 565, A69.

Melita, M.D., Licandro, J., 2012. Links between the dynamical evolution and the surface color of the Centaurs. A&A 539, A144.

Nesvorný, D., Ferraz-Mello, S., 1997. On the asteroidal population of the first-order jovian resonances. Icarus 130, 247–258.

Ohtsuka, K., Ito, T., Yoshikawa, M., Asher, D.J., Arakida, H., 2008. Quasi-Hilda comet 147P/Kushida-Muramatsu. Another long temporary satellite capture by Jupiter. A&A 489, 1355–1362.

Peixinho, N., Boehnhardt, H., Belskaya, I., Doressoundiram, A., Barucci, M.A., Delsanti, A., 2004. ESO large program on Centaurs and TNOs: visible colors - final results. Icarus 170, 153–166.

Perna, D., Dotto, E., Barucci, M.A., Mazzotta Epifani, E., Vilenius, E., Dall'Ora, M., Fornasier, S., Müller, T.G., 2013. Photometry and taxonomy of trans-Neptunian objects and Centaurs in support of a Herschel key program. A&A 554, A49.

Russell, H.N., 1916. On the albedo of the planets and their satellites. ApJ 43, 173–196.

Schleicher, D.G., Millis, R.L., Birch, P.V., 1998. Narrowband photometry of comet P/Halley: variation with heliocentric distance, season, and solar phase angle. Icarus 132, 397–417.

Schubart, J., 1968. Long-period effects in the motion of hilda-type planets. AJ 73, 99–103.

Schubart, J., 1982. Three characteristic parameters of orbits of Hilda-type asteroids. A&A 114, 200–204.

Schubart, J., 1991. Additional results on orbits of Hilda-type asteroids. A&A 241, 297–302.

Toth, I., 2006. The quasi-Hilda subgroup of ecliptic comets - an update. A&A 448, 1191–1196.

Zellner, B., Thirunagari, A., Bender, D., 1985. The large-scale structure of the asteroid belt. Icarus 62, 505–511.